23rd ABCM International Congress of Mechanical Engineering
December 6-11, 2015, Rio de Janeiro, RJ, Brazil

SPECTRAL ANALYSIS OF PRESSURE FLUCTUATIONS PRODUCED BY NUMERICAL SIMULATIONS OF A FLUIDIZED BED

Tulio Charão de Oliveira
Flávia Zinani
Maria Luiza Sperb Indrusiak
Mechanical Engineering Graduate Program, Universidade do Vale do Rio do Sinos – UNISINOS – Av. Unisinos, 950 – Cristo Rei, São Leopoldo, RS, Brazil
tuliocharao@gmail.com
fzinani@unisinos.br
mlsperb@unisinos.br

Abstract. *Fluidization is a process in which a particulate solids flow is induced by the flow of a gas or a liquid. Fluidized bed reactors are extensively used in chemical and petrochemical industries. The technology allows for more efficient and clean burning of solid fuels and also for the conversion of solid fuels into syngas by gasification. The study of hydrodynamics of fluidization is challenging and spectral analysis of pressure fluctuation measured in fluidized beds is a tool employed for the understanding and characterization of such systems. In this work, pressure fluctuation signals generated in Computational Fluid Dynamics (CFD) simulations of a fluidized bed were analyzed using Power Spectral Density (PSD) method and discrete wavelet transform method (DWT). The PSD method is based on Fast Fourier Transform (FFT) and is able to identify dominant frequencies. The DWT decomposes the signal in frequency intervals and allows the investigation of the behavior of each frequency interval in time. Three different superficial velocities were simulated in order to obtain pressure fluctuations for different fluidization regimes. It was found that 32 s of simulation with a sampling frequency of 250 Hz was sufficient to provide a signal representing all flow features. The PSD analysis showed that the dominant frequency of the process increases when the fluidization regime goes from bubbling to turbulent. The wavelet transform showed that the main flow structures occur at very low frequencies and are well captured by decomposition in six levels.*

Keywords: *wavelets, fluidized bed, pressure fluctuation, computational fluid dynamics*

1. INTRODUCTION

Fluidization is the process by which a liquid or gas flows through a particulate solid phase, keeping it under suspension, which causes the solid phase to have a fluid-like behavior. The interest in industrial applications of fluidized beds is mainly due to the large contact between the solid and gas phases during fluidization. (Kunii and Levenspiel, 1991). This technique is well known since the early nineties and became widely used since the 1970's in many processes of chemical and oil industry (Bittanti et al., 2000). However, fluidized beds became more popular in the 1980’s and 1990’s along with the increased interest in power generation using solid fuels, due to the possibility of employing low rank coal and all sorts of biomass, and also because of the minimization of pollutant emissions (Baltazar et al., 2009). Reliable mathematical models for fluidized beds are scarce yet owing to the complexity of the phenomena involved. The fundamental problem encountered in modeling hydrodynamics of a gas–solid fluidized bed is the motion of two phases where the interface is unknown and transient, and the interaction is understood only for a limited range of conditions (Gilbertson and Yates, 1996).

There are several mathematical models available for the multiphase flows which occur in fluidized beds. The numerical simulation of such systems using Computational Fluid Dynamics (CFD) must rely on models which are able to capture the desired flow features using the available computational resources. In this work, a TFM (Two fluids model) Euler-granular mathematical model was chosen, due to its relative lightness and flexibility. In this model, the mass conservation and momentum balance equations are established separately for each phase. The coupling between phases is given by two-way momentum transfer model. The solid stresses, which differ much from the conventional fluid stresses, are modeled using the Kinetic Theory of Granular Flows (KTGF) of Lun *et al.* (1984). The version implemented in the code MFIX (*https://mfix.netl.doe.gov*) has been employed in the simulations presented herein.

Experimentally, fluidized bed dynamics is usually studied through modeling and/or measuring porosity and pressure fluctuations in anywhere in the system. There is a discussion on how a calculated pressure can be compared to a measured signal in order to create a reliable representation of the fluid dynamics of the system. The type of information resulting from various ways of measuring the pressure in fluidized beds is also a point of divergence, as well as the use of absolute versus differential pressure probes (Sasic et al., 2007).

Analyses in time and frequency domains are the most common procedures for investigating the pressure signals recorded in fluidized beds. In the simple time-domain analysis, for instance, using standard deviation, the data requirements are not very strict. It is sufficient to have a pressure signal of 60 s, sampled at 20 Hz (Johnssonn *et al.*, 2000). More advanced methods of analysis in the frequency domain, e.g. a study of the probability density function (PDF) of pressure fluctuations requires considerably longer signals: more than 10 min is recommended, sampled at a frequency of 200 Hz or more. For nonparametric methods in the frequency domain, a sampling frequency of 20 Hz and a signal of typically 5 min would be enough, if one is interested only in the dynamics of large scales (bubbles). On the other hand, if finer structures are to be investigated, a significantly higher sampling frequency is needed, in general larger than 200 Hz (Sasic et al, 2007).

Pressure fluctuation data obtained from fluidized beds have been analyzed elsewhere by different methods, including standard deviation, PDFs, autocorrelation analysis and power spectral density (PSD) analysis. Standard deviation analysis has been used to identify different regimes in fluidized beds, so as to determine minimum fluidization velocity and transition between regimes (Bi et al., 1995; Zhang and Yang, 1987 and references therein). The Fourier transform has been employed for obtaining the frequencies associated with a system via analysis of the PSD of the pressure signal, aiming to identify the relation between dominant frequencies and the physical phenomena occurring in fluidized beds (Iwasaki and Matsumo, 1991; Deza and Battaglia, 2013).

Several researchers conducted experiments employing the PSD as the analysis tool (Johnsson et al., 2000, Van der Schaaf et al., 2002). The pioneers to employ the PSD analysis to pressure fluctuations predicted by CFD were Van Wachem et al. (1999) and Benyahia et al. (2000). They both used 2D TFM and reported reasonable agreement with experiments. Van Wachem *et al.* (1999) investigated PSD of CFD pressure fluctuations and void fractions of a bubbling fluidized bed (BFB). They found that the dominant frequency of the numerical pressure fluctuations were in agreement with experimental results. Their main conclusion was that Eulerian simulations are able to correctly reproduce the dynamic characteristics of laboratory-scale fluidized beds, so Eulerian CFD simulations could used as scale-up tools.

Johansson et al. (2006) used PSD analysis to compare numerical and experimental data, and concluded that the TFM based on the KTGF reproduced well the power spectra. Utikar and Ranade (2007) compared the PSD of experimental and numerical pressure fluctuations from a rectangular bed with a single jet operating in bubbling regime. The dominant frequency near the sparger was greater for the simulations than for experiments but compared well at higher locations in the bed, indicating the need of improving the values of solids properties in the KTGF. Acosta-Iborra et al. (2011) found that using a 3D domain was necessary to model a BFB to obtain good predictions for power spectra and bubble behavior compared to the experiments. Using a two-dimensional TFM for a bubbling bed, Sun et al. (2011), found that Syamlal and O'Brien drag model generated numerical results that best fitted the experimental PSD data.

Deza and Battaglia (2013) performed a numerical study (TFM of MFIX) on the hydrodynamics of BFBs of sand and a binary mixture of cotton stalks and sand, comprising bubbling ($4U_{mf}$), slugging ($6U_{mf}$) and turbulent ($8U_{mf}$) regimes. They validated their results against the experimental ones of Zhang et al. (2008, 2009). They found that standard deviation of pressure drop was over predicted for inlet velocities greater than $4U_{mf}$ when using a 2D domain; therefore, the fluidized bed was appropriately modeled by using MUSCL discretization and the Ahmadi turbulence model for velocities equal to and greater than $6U_{mf}$. For all regimes, the system behaved as a second-order dynamic one. BFBs showed one peak while slugging and turbulent beds showed two distinct peaks. It was observed that the peak at low frequency increased in magnitude as the flow transitioned from slugging to turbulent fluidization regimes. The author concluded that CFD simulations of fluidized beds with the purpose of studying pressure fluctuations are a useful tool to obtain hydrodynamic information to determine the fluidization regime.

Shou and Leu (2005) compared standard deviation with PSD and wavelet analysis to find the critical gas velocities for fluidization regime transition and found good agreement between the methods used to analyze the dynamics of the bed. Indrusiak et al. (2013) made a comparative analysis between Fourier and wavelet spectra of experimental pressure results for bubbling, slugging and turbulent fluidized beds, showing some intermittent characteristics of the phenomena. The bubbles presented themselves in the wavelet spectrum as a wake of low energy structures, with an inherent frequency of 2 Hz.

In this work, we use de PSD and wavelet decomposition methods to analyze pressure fluctuations resulting from numerical simulations of a fluidized bed based on the work of Taghipour et al. (2005).

2. METHODOLOGY

2.1 Mechanical modeling

The mathematical model employed was the one implemented in the code MFIX (Syamlal et al., 1993, Benyahia et al., 2012), which is based on an Eulerian TFM. In this model, solid and gas phases are described as interpenetrating continua mapped with respect to a fixed frame of reference. Solid phase stresses are modeled after the KTGF (Lun et al., 1984, Agrawal et al., 2001). The presence of each phase is described by its volume fraction (all phases volume fractions sum one). In this paper, only one gas phase and one solid phase are considered. As the mass and momentum governing equations are solved for each phase, the continuity equation for any phase *i*, is given by:

$$\frac{\partial}{\partial t}\left(\varepsilon_i \rho_i\right)+\nabla\cdot\left(\varepsilon_i \rho_i \mathbf{u}_i\right)=0\,, \tag{1}$$

where ε_i, ρ_i and $\mathbf{u}_i$ are the volume fraction, density, and velocity for each phase i. The momentum equation for the gas phase, g, and solid phase, s, are given by:

$$\frac{\partial}{\partial t}\left(\varepsilon_g \rho_g \mathbf{u}_g\right)+\nabla\cdot\left(\varepsilon_g \rho_g \mathbf{u}_g \mathbf{u}_g\right)=\nabla\cdot\boldsymbol{\tau}_g-\varepsilon_g\nabla P+\varepsilon_g \rho_g \mathbf{g}-\mathbf{I}\,, \tag{2}$$

$$\frac{\partial}{\partial t}\left(\varepsilon_s \rho_s \mathbf{u}_s\right)+\nabla\cdot\left(\varepsilon_s \rho_s \mathbf{u}_s \mathbf{u}_s\right)=\nabla\cdot\boldsymbol{\tau}_s-\varepsilon_s\nabla P+\varepsilon_s \rho_s \mathbf{g}+\mathbf{I}\,, \tag{3}$$

In the left hand sides the material derivatives represent the rate of change of momentum, while in the right hand sides the superficial forces are given by the gas pressure, P, and by the extra stress tensor, $\boldsymbol{\tau}$, of each phase (g for gas and s for solid). The body forces are given by vector $\mathbf{g}$ and $\mathbf{I}$ is the vector of interaction forces which result from momentum transfer between phases. The latter is given as $\mathbf{I} = \beta(\mathbf{u}_g - \mathbf{u}_s)$, where the drag coefficient β is usually calculated by a correlation. In this work, the Gidaspow model is employed (Gidaspow, 1994). In this model, the dense phase ($\varepsilon_s > 0.2$) is modeled using Ergun equation (Ergun, 1952) and the disperse phase ($\varepsilon_s \leq 0.2$) using Wen and Yu model (Wen and Yu, 1966). The gas phase is treated as an ideal gas with newtonian viscosity. As the solid phase stresses are modeled after the KTGF, an additional primal variable must be solved in order to close the problem. This variable is the granular temperature, Θ, which is the result of solid velocity fluctuations. The granular temperature is the basis for the modeling of the solid stress tensor and solid pressure. Its balance equation is given as:

$$\frac{3}{2}\left[\frac{\partial}{\partial t}\left(\rho_s \varepsilon_s \Theta_s\right)+\nabla\left(\rho_s \varepsilon_s \mathbf{u}_s \Theta_s\right)\right]=\left(-p_s \mathbf{I}+\boldsymbol{\tau}_s\right):\nabla\mathbf{u}_s+\nabla\cdot\left(k_{\Theta s}\nabla\Theta_s\right)-\gamma_{\Theta gs}+\phi_{gs}\,, \tag{4}$$

where the first term on the right hand side is the generation of energy by the solid stress tensor, the second term is the diffusive term, in which $k_{\Theta s}$ is the granular temperature diffusion coefficient, the third term is the dissipation due collisions term, accounted by $\gamma_{\Theta s}$, and $\phi_{\gamma s}$ accounts for energy transfer between gas and solid phases. Further details on this model may be found in the "Summary of MFIX Equations 2012-1" by Benyahia et al. (2012) and in the MFIX theory guide (Syamlal et al., 1993).

2.2 PSD

The Power Spectral Density (PSD) is a method to analyze the energy content of a signal associated with to the frequencies of a physical phenomenon (Bendat and Piersol, 2010). The power spectral density function, P_{yy}, or power spectrum can be computed as:

$$P_{yy}\left(f\right)=\left|Y\left(f\right)\right|^2 \tag{5}$$

where $Y(f)$ are the coefficients of the Fourier transform of the time series $y(t)$.

2.3 DWT

The presence of bursts or transient phenomena may or may not be observed in physical space, but will be completely hidden in the Fourier space, since the transform coefficients refer to the entire time domain of the signal. The Fourier transform base components - the sine and cosine functions- have infinite support, i.e. they are located in frequency, but extend over the whole time domain. Therefore the coefficients represent an average for the entire domain at each frequency considered.

The wavelet transform allows a time location along with frequency analyses. The bases of the wavelet transform are located both in frequency and time domain and due to this property of dual location, there is a balance in the resolutions in each area: the gain in temporal resolution is offset by a loss of resolution in frequency, according to the Heisenberg's uncertainty principle. This fact does not represent a limitation of the perception or of the analysis tools, but follows from the definition of frequency, which may not be measured instantaneously.

The bases of wavelet transforms are generated through dilations and translations of a single wavelet function $\psi(t)$:

$$\psi_{a,b}(t)=\frac{1}{\sqrt{a}}\ \psi\left(\frac{t-b}{a}\right),\quad a,b\in R,\quad a>0 \tag{6}$$

where a and b are respectively the scale and position coefficient. The discretization of the bases can be done overwriting in Eq. (1) the scale coefficient a by 2^j and the position coefficient b by $k2^j$, with $(j, k) \in I$. The discrete wavelet transform (DWT) is thus given by:

$$\tilde{X}(j,k)=\sum_t x(t)\psi_{j,k}(t)\qquad j,k\in \mathrm{I} \tag{7}$$

In practice, the DWT of a series with more than 2^J elements is computed for $1 \le j \le J$, being J a convenient arbitrary choice. The remaining part of the signal, containing the mean values for a scale J, is given by:

$$\tilde{X}(J,k)=\sum_t x(t)\phi_{J,k}(t) \tag{8}$$

where $\phi(t)$ is the scale function associated to the wavelet function. Then, any discrete time series with a sampling frequency Fs can be represented by:

$$x(t)=\sum_k \tilde{X}(J,k)\phi_{J,k}(t)+\sum_{j\le J}\sum_k \tilde{X}(j,k)\psi_{j,k}(t) \tag{9}$$

where the first term is the approximation of the signal at the scale J, which corresponds to the frequency interval $[0, Fs/2^{J+1}]$ and the inner summation of the second term are details of the signal at the scales j ($1 \le j \le J$), which corresponds to frequency intervals $[Fs/2^{j+1}, Fs/2^j]$.

2.4 Problem statement and numerical model

The fluidized bed employed in the numerical simulations was based on the work of Taghipour et al. (2005). It has a rectangular base of 0.28 m x 0.025 m and height of 1 m, as shown in Fig. 1(a). A 3D mesh consisting of 11,200 hexahedral cells with Δx = 0.5 cm was built. The boundary conditions were of gas uniform superficial velocity, U_0, at the bottom - three values were considered, $6U_{mf}$, $7U_{mf}$ and $12U_{mf}$, for the experimental minimum fluidization velocity, U_{mf}, equal to 0,065 m/s. At the top, a pressure outlet boundary condition was imposed. At the walls, no-slip condition was imposed for the gas phase while partial slip (Johnson and Jackson, 1987) was imposed for the solid phase. In the initial condition, settled particles, with 0.4 voidage, occupy the bed to a height of 0.4 m. From 0.4 m to 1 m the domain is occupied by air. The air velocity in the bed is a ratio of the superficial velocity to the voidage, and above the bed it is equal to the superficial velocity. The particles were assumed to be perfectly spherical, with diameter equal to 275 μm and density equal to 2500 kg/m^3. The fluidization agent was air at the temperature of 20 ºC. The pressure fluctuations were acquired at two virtual probes, situated at 0.04 m and 0.35 m above the distributor, as shown in Fig. 1(b). According to the correlations of Bi and Grace (1995), the superficial velocities of $6U_{mf}$ and $7U_{mf}$ should cause bubbling regime while for $U_0 = 12U$mf, the turbulent regime should be expected.

According to Sasic et al. (2007), the absolute pressure signal contains a great amount of information about the flow, such as pressure waves, bubble traveling and bursting, while the differential pressure signal only give information about phenomena registered between the pressure taps, such as the passage of bubbles and clusters. So, the absolute pressure signal was chosen to be analyzed with spectral methods described in this work.

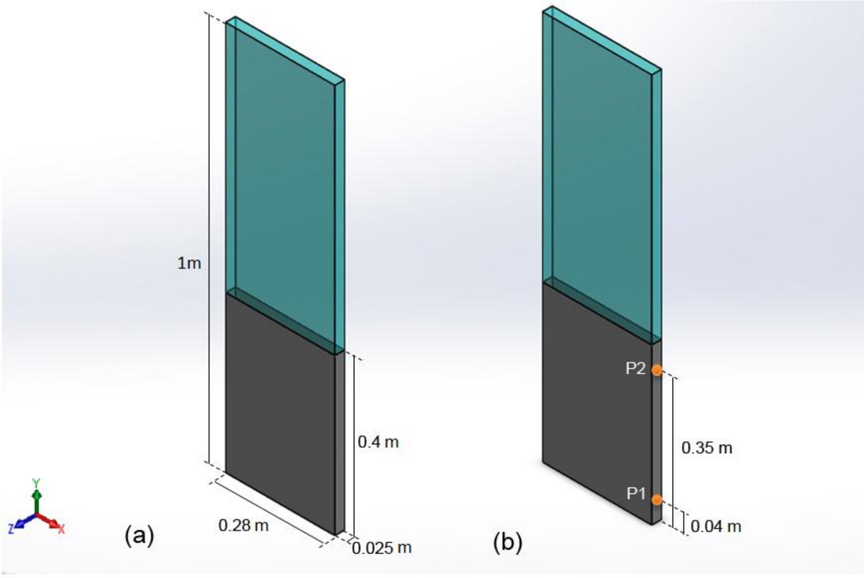

Figure 1: Bed dimensions and pressure probe positions.

3. RESULTS AND DISCUSSION

3.1 Sampling frequency and simulation time

The first step was to determine the sampling frequency and the time of simulation needed to obtain signals that could represent the phenomena occurring in a steady-state regime with statistical significance. With this purpose, the simulations were conducted for a period of time of 132 s and acquisition frequency of 1000 Hz. Then the pressure signals were subsampled in periods of 65 s and 31 s and sampling rates of 500 Hz and 250 Hz. It was found that 31 s of simulation with sampling frequency of 250 Hz could give the same information as higher periods and frequencies. in Fig. 2, the PSD analysis of the pressure signal obtained at P2 for $U_0 = 7U_{mf}$. It is possible to observe that the peaks in the PSD are the same for all frequencies (Fig. 2(a)) of simulation times employed (Fig. 2(b)).

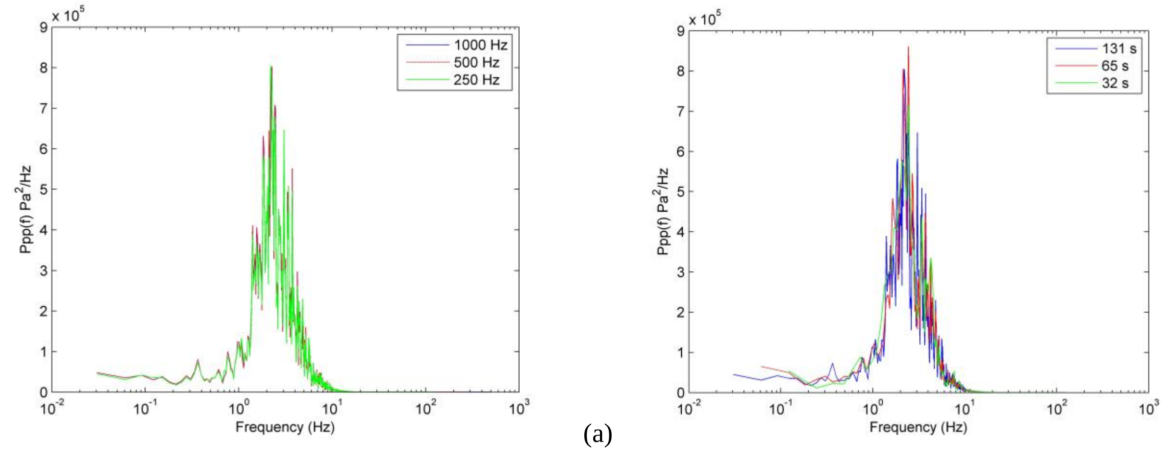

Figure 2: PSD for different (a) sampling rates and (b) simulation times.

3.2 PSD analyses

The PSD analyses for the three superficial velocities investigated showed that there are major differences on the PSD spectrum when the fluidization undergoes different regimes. Point P2 was investigated with more emphasis in view that signals obtained farther from the distributor are more suitable to give information about the flow (Sasic et al., 2007). The power spectrum for $U_0 = 6U_{mf}$ is shown in Fig. 3(a). It is possible to identify a dominant frequency of about 2.56 Hz, as indicated by the arrow. In Fig. 3(b) the power spectrum for $U_0 = 12U_{mf}$ is depicted. In this case three close peaks are identified, one at 2.32 Hz and others at 2.93 Hz and 3.91 Hz.

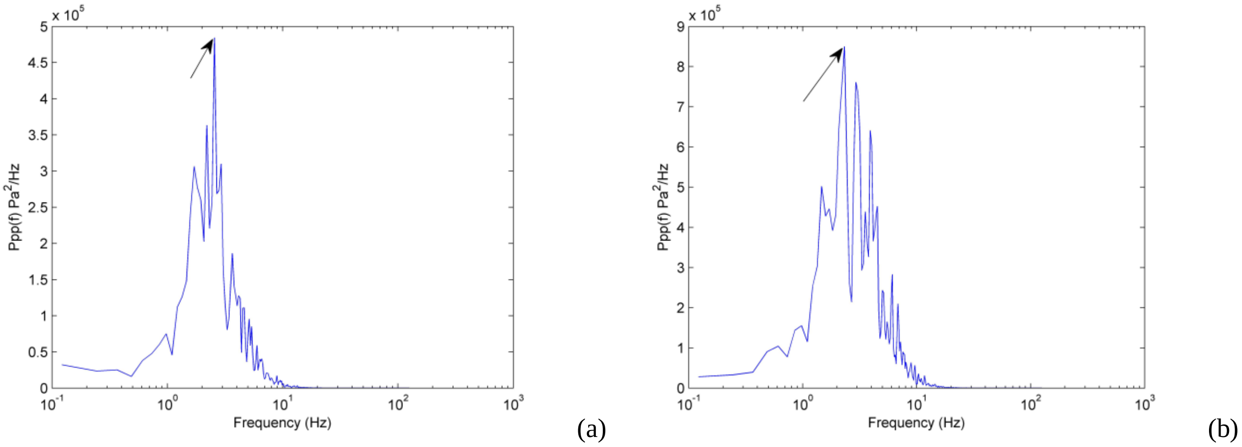

Figure 3. PSD Analyses. (a) $U_0 = 6U_{mf}$ and (b) $U_0 = 12U_{mf}$.

Figure 4 shows instantaneous gas volume fraction fields for (a) $U_0 = 6U_{mf}$, (b) $U_0 = 7U_{mf}$ and (c) $U_0 = 12U_{mf}$, showing that the (a) was under bubbling regime while (c) was under turbulent regime, which explains the difference between the power spectra. The dominant frequency when $U_0 = 6U_{mf}$ is probably the frequency of bubbles detachment, while in the turbulent regime the flow is more chaotic and there are important phenomena not only in one frequency.

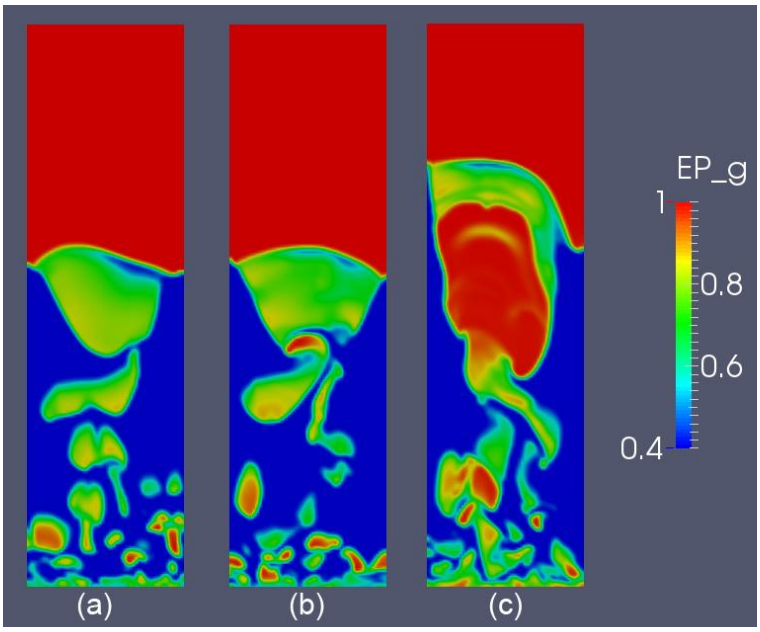

Figure 4. Instantaneous gas volume fraction profiles. (a) $U_0 = 6U_{mf}$, (b) $U_0 = 7U_{mf}$ and (c) $U_0 = 12U_{mf}$.

3.3 DWT analyses

Wavelet analyses using DWT were performed, employing six levels to obtain a good representation of the dominant frequencies of the flows. The wavelet decomposition works as a low pass filter, extracting from the signal the high frequency components and stressing the signal behavior at low frequencies. Approximations from level 1 to 6 were employed, to find in approximation a6 a frequency range from 0 Hz to 3.91 Hz. This range comprises the dominant ones found for the bubbling and turbulent regimes.

Figure 5(a) depicts the decomposition of the pressure signal at P2 for $U_0 = 6U_{mf}$, while Fig. 5(b) depicts the decomposition of the pressure signal at P2 for $U_0 = 12U_{mf}$. The greatest frequency shown is of 31.25 Hz, because the first decomposition levels (d1 - d3) did not show important values. It is also possible to see that the signal shown in d4 achieves much higher levels for the turbulent case, $U_0 = 12\ U_{mf}$ in Fig. 5(b). The signals detailed in a6, for the lowest frequencies, suggest that there may be a flow feature which is modifying the low-frequency phenomena with a period of about 5 seconds.

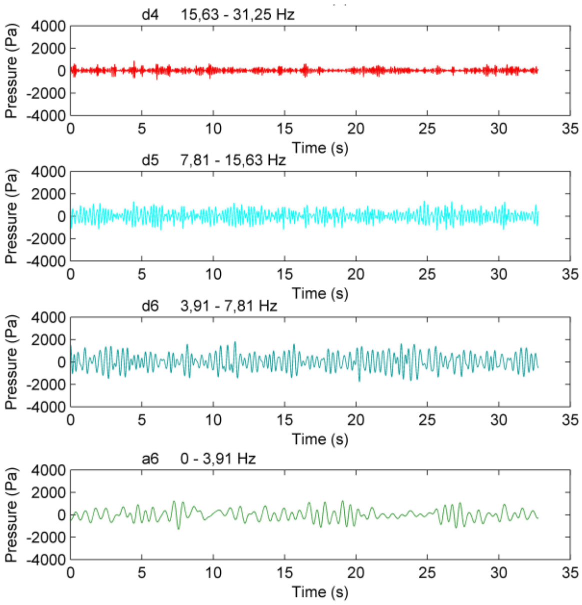

(a)

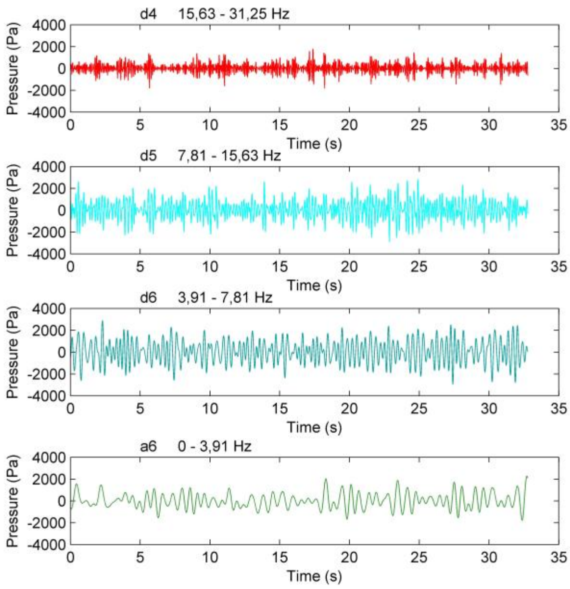

(b)

Figure 5. Wavelets decomposition of the pressure signal at P2 for (a) $U_0 = 6U_{mf}$ and (b) $U_0 = 12U_{mf}$.

4. ACKNOWLEDGEMENTS

The authors acknowledge CNPq and CAPES for funding. The author F. Zinani is a grant holder of CNPq.

5. REFERENCES

Acosta-Iborra, A. et al., 2011. “Experimental and computational study on the bubble behavior in 3d fluidized bed”, *Chemical Engineering Science*, Vol. 66, p. 3499-3512.

Agrawal, K. et al., 2001. “The role of meso-scale in rapid gas-solid flows”, *Journal of Fluid Mechanics*, Vol. 445, p. 151-185.

Baltazar, A. W. S. et al., 2009. “Simulação transiente de um reator de leito fluidizado em 3D”. *REM: Revista Escola de Minas*, Vol. 62, p. 59-64.

Bendat, J.S. and Piersol, A.G., 2010. *Random data: analysis and measurement procedures*. Wiley Interscience, New York, 4th edition.

Benyahia, S. et al., 2000. “Simulation of particles and gas flow behavior in the riser section of a circulating fluidized bed using the kinect theory approach for the particulate phase”, *Powder Technology*, Vol. 112, p. 24-33.

Benyahia, S. et al., 2012. “Summary of MFIX Equations 2012-1”. 4 May 2015 <https://mfix.netl.doe.gov/documentation/MFIXEquations2012-1.pdf>.

Bi, H. T. and Grace, J. R., 1995. “Flow Regime Diagrams for Gas-Solid Fluidization and Upward Transport”, *International Journal of Multiphase Flow*, Vol. 21, p. 1229-1236.

Bi, H.T. et al., 1995. “Regime Transitions Affecting Gas-Solids Suspensions And Fluidized Beds”, *Chemical Engineering Research and Design*, Vol. 73, p. 154-161.

Bittanti, S. et al., 2000. “A model of a bubbling fluidized bed combustor oriented to char mass estimation”, *IEEE Transactions on control systems technology*, Vol. 8, p. 247-256.

Deza, M., and Battaglia, F., 2013. “A CFD Study of Pressure Fluctuations to Determine Fluidization Regimes in Gas-Solid Beds”, *Journal of Fluids Engineering, Blacksburg*, Vol. 135.

Ergun, S., 1952. “Flow through Packed Columns”, *Chemical Engineering Progress*, Vol. 48, p. 89.

Gidaspow, D., 1994. *Mutliphase Flow and Fluidization: Continuum and Kinetic Theory Descriptions*, Academic Press, 1st edition.

Gilbertson, M. A. and Yates, J. G., 1996. “The motion of particles near a bubble in a gas-fluidized bed”, *Journal of Fluid Mechanics*, Vol. 323, p. 377-385.

Indrusiak, M. L. S. et al., 2013. “Wavelet Characterization of the Flow Regime in a Gas-Solid Fluidized Bed”, *Journal of Energy and Power Engineering*, n. 7, p. 1023-1031.

Iwasaki, H. K. N. and Matsumo, H. Y. Y., 1991. "Frequency analysis of pressure fluctuation in fluidized bed plenum", *Journal of Chemical Engineering Reactors*, Vol. 7, p. 1-29.

Johansson, K. et al., 2006. “Experimental validation of CFD models for fluidized beds: influence of particle stress models, gas phase compressibility and air inflow models”, *Chemical Engineering Science*, Vol. 61, p. 1705-1717.

Johnsson, F. et al., 2000. "Characterization of Fluidization Regimes by Time-Series Analysis of Pressure Fluctuations". *International Journal of Multiphase Flow*, n. 26, p. 663-715.

Johnson, P.C. and Jackson, R., 1987. "Frictional-collision constitutive relations for granular materials with application to plane shearing". *Journal of Fluid Mechanics*, Vol. 176, p. 67-93.

Kunii, D. and Levenspiel, O., 1991. *Fluidization Engineering* , Butterworth-Heinemann, Newton, 2nd edition.

Lun, C. K. K. et al., 1984. "Kinetic theories for granular flow: inelastic particles in Couette flow and slightly inelastic particles in a general flow field", *Journal of Fluid Mechanics*, Vol. 140, p. 223-256.

Sasic, S. et al., 2007. "Characterization of fluid dynamics of fluidized beds by analysis of pressure fluctuations", *Progress in Energy and Combustion Science*, n. 33, p. 453-496.

Shou, MC and Leu, LP., 2005. "Energy of power spectral density function and wavelet analysis of absolute pressure fluctuation measurements in fluidized beds", *Chemical Engineering Research & Design*, Vol. 83, p.478-491.

Sun, J. et al., 2011. "CFD simulation and experiments of dynamics parameters in gas-solid fluidized bed", *Chemical Engineering Science*, Vol. 66, p. 4972-4982.

Syamlal, M. et al., 1993. "MFIX Documentation Theory Guide". 4 May 2015. <https://mfix.netl.doe.gov/download/mfix/mfix_legacy_manual/Theory.pdf>.

Taghipour, F. et al., 2005. "Experimental and computational study of gas–solid fluidized bed hydrodynamics", *Chemical Engineering Science*, n. 60, p. 6857-6867.

Utikar, R. P. and Ranade, V. V., 2007. "Single jet fluidized beds: experiments and CFD simulations with glass and polypropylene particles", *Chemical Engineering Science* Vol. 62, p. 167-183.

Van Der Schaaf, J. et al., 2002. "Non-intrusive determination of bubble and slug length scales in fluidized beds by decomposition of the power spectral density of pressure time series", *International Journal of Multiphase Flow*, Vol. 28, p. 865-880.

Van Wachem, B. G. M. et al., 1999. "Validation of the Eulerian simulated dynamic behaviour of gas-solid fluidized beds", *Chemical Engineering Science*, Vol. 54, p. 2141-2149.

Wen, C. Y. and Yu, Y. H., 1966. "A generalized method for predicting the minimum fluidization velocity". *AIChE Journal*, Vol. 12, p. 610-612.

Zhang, M. C. and Yang, R.Y.K., 1987. "On The Scaling Laws For Bubbling Gas- Fluidized Bed Dynamics", *Powder Technology*, n. 2, p. 51-159.

Zhang, Y. et al., 2008. "Fluidization, Mixing and Segregation of Biomass–Sand Mixture in a Fluidized Bed", *International Journal of Chemical Reactor Engineering*, Vol. 6, p. 1–29.

Zhang, Y. et al., 2009. "Characterization of Fluidization and Segregation of Biomass Particles by Combining Image Processing and Pressure Fluctuation Analysis", *International Journal of Chemical Reactor Engineering*, Vol. 7, p. 1–19.

6. RESPONSIBILITY NOTICE

The authors are the only responsible for the printed material included in this paper.